NATURAL CONVECTION IN AN INCLINED SQUARE ENCLOSURE CONTAINING INTERNAL ENERGY SOURCES

Md. Tofiqul Islam*, Sumon Saha and Md. Arif Hasan Mamun
Department of Mechanical Engineering
Bangladesh University of Engineering and Technology (BUET), Dhaka-1000, Bangladesh.
*Corresponding address: mtislam@me.buet.ac.bd
Goutam Saha
Department of Related Subjects, Ahsanullah University of Science and Technology (AUST),
Dhaka-1215, Bangladesh

Abstract: *Natural convection in an inclined differentially heated square enclosure containing internally heated fluid has been investigated numerically using the Galerkin finite element method. The horizontal walls are adiabatic, while the side walls are isothermal but kept at different temperatures. Flow and heat transfer characteristics through isotherms, streamlines and average Nusselt numbers have been presented for the external Rayleigh number 10^3 to 10^6, internal Rayleigh number 10^5 to 10^8 and inclination angles 0º to 30º. The obtained computational results indicate that the strength of the convective currents depends on the internal energy. Heat removal rate is optimized at zero inclination angle for relatively weak external heating mode for all values of internal energy.*

Keywords: *Natural convection, finite element method, square enclosure, Rayleigh number.*

INTRODUCTION

During the last four decades, significant attention was given to the study of natural convection in enclosures subjected to simultaneous volumetric internal heat generation and external heating or cooling. This was due to the occurrence of natural convection in a wide range of application areas that include nuclear reactor design, post-accident heat removal in nuclear reactors, geophysics and underground storage of nuclear waste, energy storage systems and others. Literature review shows various studies have been published on the mechanism of natural convection in heated enclosure containing heat generating fluids with different geometrical parameters and boundary conditions.

The published literature dealing with externally heated enclosures has been reviewed by Ostrach[1] and also by Catton[2]. The literature related to internally heated enclosures had been compiled by Kulack et al.[3]. Baker et al.[4] and Cheung[5] examined the available data for both internally heated layers with equal upper and lower boundary temperatures and internally heated layer with insulated lower boundary, and have presented correlation for internally heated layers with unequal boundary temperatures. Kikuehi et al.[6] and Boon-Long et al.[7] investigated experimentally the heat transfer behavior in a horizontal layer with simultaneous internal and external heating. Suo-Anttilla and Catton[8] used the Landau method to determine the heat transfer in a horizontal, internally heated layer which is cooled from below and then conducted an experimental study of the same problem[9].

Steinberner and Reinke[10] performed experiments with a rectangular geometry of both the upper and lower walls being cooled for Ra_I varying from 5×10^{10} to 3×10^{13}. Based on a numerical modeling effort, they developed correlation for the Nusselt number. Kulacki and Goldstein[11] experimentally measured heat transfer from a plane layer containing internal energy sources with equal boundary temperature. Lee and Goldstein[12] performed a laboratory experiment similar to that performed by Kulacki and Goldstein but they employed an inclined square enclosure. Acharya and Goldstein[13] presented a numerical solution of natural convection in the externally heated square boxes of different aspect ratios and containing internal energy sources. Their study covered Ra_I from 10^4 to 10^7 and Ra_E from 10^3 to 10^6, and enclosure inclination

---

Nomenclature

g	gravitational acceleration [m/s^2]
k	thermal conductivity [W/m^2.K]
L	length of the heat source [m]
Nu	Nusselt number
p	pressure [Pa]
P	dimensionless pressure
Pr	Prandtl number
Q	internal volumetric heat generation
Ra_I	internal Rayleigh number
Ra_E	external Rayleigh number
T	temperature [K]
u, v	dimensional velocity [m/s]
U, V	dimensionless velocity
x, y	dimensional coordinates
X, Y	non-dimensional coordinates

Greek symbols

Φ	inclination angle [deg]
α	thermal diffusivity [m^2/s]
β	thermal expansion coefficient [1/K]
η	kinematic viscosity [m^2/s]
θ	dimensionless temperature
ρ	fluid density [kg/m^3]

Subscripts

c	cold wall
H	hot wall
o	average

angle from 30° to 90°. They found that the flow pattern is related to the ratio Ra_E / Ra_I. Emara and Kulacki[14] reported a numerical study of thermal convection in a fluid layer driven by uniform volumetric energy sources. The sides and lower surfaces of the rectangular domain were adiabatic walls and the upper surface was either rigid or free isothermal boundary. Rahman and Sharif[15] conducted a numerical investigation for free convective laminar flow of a fluid with or without internal heat generation ($Ra_E = Ra_I = 2 \times 10^5$) in rectangular enclosures of different aspect ratios (from 0.25 to 4), at various angles of inclination, of insulated side walls, heated bottom, and cooled top walls. They observed that for $Ra_E / Ra_I > 1$, the convective flow and heat transfer were almost the same as that in a cavity without internal heat generating fluid. Kawara et al.[16] performed experimental study on natural convection in a differentially heated vertical fluid layer of $Pr = 5.85$ with internal heating. Fusegi et al.[17] reported a numerical study on natural convection in square cavity with uniform internal heat generation and differentially heated vertical sidewalls. Fusegi et al. [18] also generated results for the same problem but considering a rectangular cavity of different aspect ratios. These works of Fusegi et al. involved high external Rayleigh number $Ra_E = 5 \times 10^7$ and internal Rayleigh number $Ra_I = 10^9$ to 10^{10}. Their results agreed with the experimental results of Kawara et al. Oztop and Bilgen[19] numerically studied a differentially heated, partitioned, square cavity containing a heat generating fluid. The vertical walls were isothermal while the horizontal walls were adiabatic and an isothermal cold partition was attached to the bottom wall. The external and internal Rayleigh numbers (i.e. Ra_E and Ra_I) ranged from 10^3 to 10^6. They observed two distinct flow regimes based on the ratio Ra_E / Ra_I. Shim and Hyun[20] presented the time-dependent behavior of natural convection in a differentially heated square cavity due to impulsively switched on uniform internal heat generation. They concluded that as the transient behavior is dependent on Ra_E / Ra_I , three flow stages were distinguished.

Baytas[21] investigated the effect of the uniformly distributed sinusoidal heat source generation on the fluid flow and heat transfer within a two-dimensional square cavity. Liaqat and Baytas[22] studied the conjugate natural convection in a square enclosure containing uniform volumetric sources and having thick conducting walls. They illustrated the importance of performing conjugate investigations instead of conventional non-conjugate analyses. For a fluid layer, with a lower wall adiabatic and upper wall maintained at a constant temperature along with constant volumetric generation in the fluid, Kulacki and Goldstein[23] obtained the critical Rayleigh number, for the transition from the conduction to the convection regime. In this analysis, the critical Rayleigh number was obtained using two methods. The first approach followed the linear theory by Rayleigh, discussed in Drazin and Reid[24], and the second approach was based on the energy method. May[25] solved the problem of transient natural convection using the stream function vorticity method. He reported that the periodic solution exists for $Ra > 5 \times 10^4$. Piazza et al.[26] and Arcidiacono et al.[27-28] analyzed low Prandtl number natural convection flows, using the finite volume technique. By successively increasing the Grashof number, they obtained steady, periodic, and chaotic solutions. Relatively less literature is available for the study of volumetrically heated cavities using analytical methods. Daniels and Jones[29] considered a long cavity, whereas a similar approach was used by Joshi et al.[30] for a tall cavity.

The aim of this paper is to examine the steady natural convection inside a square tilted cavity consisting of two horizontal straight adiabatic walls and two vertical walls, which are at constant but different temperature. The numerical results have been obtained by solving the governing equations using the Galerkin finite element method. The effects of internal energy, the external energy and the inclination angles on the thermo-fluid characteristics in the square titled enclosure filled with a uniform heat generating fluid have been analyzed. Selection of the optimum titled position of the square cavity, for which better convective heat transfer has been obtained in between the combined effects of Ra_I and Ra_E, has also been performed.

PROBLEM DEFINITION

Schematic diagram of the problem with coordinate system and boundary conditions are shown in Fig. 1. It consists of a square enclosure whose left vertical wall is

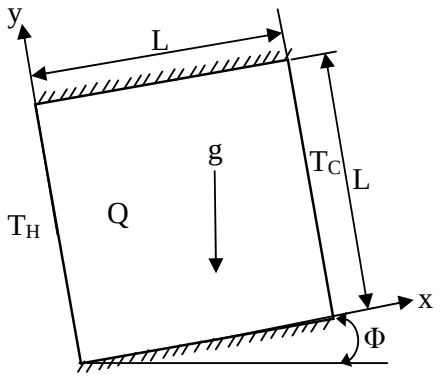

Fig. 1: Schematic diagram of the physical domain

maintained at a temperature T_H while the right vertical wall is held at a temperature T_C and top and bottom walls are kept adiabatic. It is filled with a uniform heat generating fluid with volumetric rate of Q. The flow and attendant heat transfer are characterized by the externally controllable Rayleigh number $Ra_E = (\beta g \Delta t L^3)/(\eta\alpha)$ and the Prandtl number $Pr = \eta/\alpha$. Here, Δt denotes the imposed temperature difference between the two sidewalls ($\Delta t = T_H - T_C$). The introduction of internal heat generation is represented by the internal Rayleigh number $Ra_I = (\beta g Q L^3)/(\eta\alpha)$.

MATHEMATICAL MODEL

It is assumed that the fluid is Newtonian and incompressible, the flow is laminar and the effect of viscous dissipation is negligible. The Boussinesq approximation is invoked for the fluid properties to relate density changes to temperature changes, and to couple in this way the temperature field to the flow field. Then the governing equations for steady natural convection can be expressed in the dimensionless form as:

$$\frac{\partial U}{\partial X} + \frac{\partial V}{\partial Y} = 0 \tag{1}$$

$$U\frac{\partial U}{\partial X} + V\frac{\partial U}{\partial Y} = -\frac{\partial P}{\partial X} + \left(\frac{\partial^2 U}{\partial X^2} + \frac{\partial^2 U}{\partial Y^2}\right) + \left(\frac{Ra_E}{Pr}\sin\Phi\right)\theta \tag{2}$$

$$U\frac{\partial V}{\partial X}+V\frac{\partial V}{\partial Y}=-\frac{\partial P}{\partial Y}+\left(\frac{\partial^2 V}{\partial X^2}+\frac{\partial^2 V}{\partial Y^2}\right)+\left(\frac{Ra_E}{Pr}\cos\Phi\right)\theta \quad (3)$$

$$U\frac{\partial \theta}{\partial X}+V\frac{\partial \theta}{\partial Y}=\frac{1}{Pr}\left(\frac{\partial^2 \theta}{\partial X^2}+\frac{\partial^2 \theta}{\partial Y^2}\right)+\left(\frac{Ra_I}{Ra_E\,Pr}\right) \quad (4)$$

The dimensionless parameters in the equations above are defined as follow:

$$X=\frac{x}{L},\ Y=\frac{y}{L},\ U=\frac{u\,L}{\eta},\ V=\frac{v\,L}{\eta},$$

$$P=\frac{p\,L^2}{\rho\eta^2},\ \theta=\frac{T-T_o}{T_H-T_C},\ T_o=\frac{T_H+T_C}{2}.$$

The major dimensionless parameters explicitly appearing in the equations are the previously defined Ra_E, Ra_I, and Pr. The boundary conditions for the present problem are specified as follows:

All the walls of the cavity	$U = 0, V = 0$
Bottom and top walls	$\frac{\partial \theta}{\partial Y} = 0$
Right side wall	$\theta = -0.5$
Left side wall	$\theta = 0.5$

The heat transfer parameter of interest is defined as below.

$$Nu=\int_0^1\left(\frac{\partial \theta}{\partial X}\right)_{X=0}dY$$

FINITE ELEMENT FORMULATION

The velocity and the temperature distributions and linear interpolation for the pressure distribution according to their highest derivative orders in the differential Eqs. (1)-(4) as

$$U(X,Y)=N_\alpha U_\alpha,\ V(X,Y)=N_\alpha V_\alpha,$$

$$\theta(X,Y)=N_\alpha \theta_\alpha,\ P(X,Y)=H_\lambda P_\lambda.$$

where α = 1, 2, 3, … …, 9; λ= 1, 2, 3; N_α are the element interpolation functions for the velocity components and the temperature, and H_λ are the element interpolation functions for the pressure. To derive the finite element equations, the method of weighted residual is applied to the Eqs. (1)-(4) to get

$$\int_A N_\alpha\left(\frac{\partial U}{\partial X}+\frac{\partial V}{\partial Y}\right)dA=0 \quad (5)$$

$$\int_A N_\alpha\left(U\frac{\partial U}{\partial X}+V\frac{\partial U}{\partial Y}\right)dA=-\int_A H_\lambda\left(\frac{\partial P}{\partial X}\right)dA+\int_A N_\alpha\left(\frac{\partial^2 U}{\partial X^2}+\frac{\partial^2 U}{\partial Y^2}\right)dA+\int_A N_\alpha\left(\frac{Ra_E}{Pr}sin\Phi\right)\theta\,dA \quad (6)$$

$$\int_A N_\alpha\left(U\frac{\partial V}{\partial X}+V\frac{\partial V}{\partial Y}\right)dA=-\int_A H_\lambda\left(\frac{\partial P}{\partial Y}\right)dA+\int_A N_\alpha\left(\frac{\partial^2 V}{\partial X^2}+\frac{\partial^2 V}{\partial Y^2}\right)dA+\int_A N_\alpha\left(\frac{Ra_E}{Pr}\cos\Phi\right)\theta dA \quad (7)$$

$$\int_A N_\alpha\left(U\frac{\partial \theta}{\partial X}+V\frac{\partial \theta}{\partial Y}\right)dA=\frac{1}{Pr}\int_A N_\alpha\left(\frac{\partial^2 \theta}{\partial X^2}+\frac{\partial^2 \theta}{\partial Y^2}\right)dA+\frac{Ra_I}{Ra_E\,Pr}\int_A N_\alpha dA \quad (8)$$

where A is the element area. Gauss's theorem is then applied to Eqs. (6)-(8) to generate the boundary integral terms associated with the surface tractions and heat flux. Then Eqs. (6)-(8) become,

$$\int_A N_\alpha\left(U\frac{\partial U}{\partial X}+V\frac{\partial U}{\partial Y}\right)dA+\int_A H_\lambda\left(\frac{\partial P}{\partial X}\right)dA+\int_A\left(\frac{\partial N_\alpha}{\partial X}\frac{\partial U}{\partial X}+\frac{\partial N_\alpha}{\partial Y}\frac{\partial U}{\partial Y}\right)dA-\int_A\left(\frac{Ra_E}{Pr}\sin\Phi\right)N_\alpha\theta\,dA=\int_{S_0}N_\alpha S_x dS_0$$

$$\int_A N_\alpha\left(U\frac{\partial V}{\partial X}+V\frac{\partial V}{\partial Y}\right)dA+\int_A H_\lambda\left(\frac{\partial P}{\partial Y}\right)dA+\int_A\left(\frac{\partial N_\alpha}{\partial X}\frac{\partial V}{\partial X}+\frac{\partial N_\alpha}{\partial Y}\frac{\partial V}{\partial Y}\right)dA-\int_A\left(\frac{Ra_E}{Pr}\cos\Phi\right)N_\alpha\theta\,dA=\int_{S_0}N_\alpha S_y dS_0$$

$$\int_A N_\alpha\left(U\frac{\partial \theta}{\partial X}+V\frac{\partial \theta}{\partial Y}\right)dA+\frac{1}{Pr}\int_A\left(\frac{\partial N_\alpha}{\partial X}\frac{\partial \theta}{\partial X}+\frac{\partial N_\alpha}{\partial Y}\frac{\partial \theta}{\partial Y}\right)dA=\int_{S_w}N_\alpha q_w dS_w+\frac{Ra_I}{Ra_E\,Pr}\int_A N_\alpha dA$$

Here Eqs. (5)-(7) specify surface tractions (S_x, S_y) along outflow boundary S_0 and Eq. (8) implies velocity components and fluid temperature or heat flux that flows into or out from domain along wall boundary S_w. Substituting the element velocity component distributions, the temperature distribution, and the pressure distribution, the finite element equations can be written in the form,

$$K_{\alpha\beta^x}U_\beta+K_{\alpha\beta^y}V_\beta=0 \quad (9)$$

$$K_{\alpha\beta\gamma^x}U_\beta U_\gamma+K_{\alpha\beta\gamma^y}V_\gamma U_\gamma+M_{\alpha\mu^x}P_\mu+\left(S_{\alpha\beta^{xx}}+S_{\alpha\beta^{yy}}\right)U_\beta-\left(\frac{Ra_E}{Pr}sin\Phi\right)K_{\alpha\beta}\theta_\beta=Q_{\alpha^u} \quad (10)$$

$$K_{\alpha\beta\gamma^x}U_\beta V_\gamma+K_{\alpha\beta\gamma^y}V_\gamma V_\gamma+M_{\alpha\mu^y}P_\mu+\left(S_{\alpha\beta^{xx}}+S_{\alpha\beta^{yy}}\right)V_\beta-\left(\frac{Ra_E}{Pr}cos\Phi\right)K_{\alpha\beta}\theta_\beta=Q_{\alpha^v} \quad (11)$$

$$K_{\alpha\beta\gamma^x}U_\beta\theta_\gamma+K_{\alpha\beta\gamma^y}V_\beta\theta_\gamma+\frac{1}{Pr}\left(S_{\alpha\beta^{xx}}+S_{\alpha\beta^{yy}}\right)\theta_\beta-\frac{Ra_I}{Ra_E\,Pr}K_\alpha=Q_{\alpha^\theta} \quad (12)$$

where the coefficients in element matrices are in the form of the integrals over the element area and along the element edges S_0 and S_w as,

$$K_{\alpha\beta^x}=\int_A N_\alpha N_{\beta,x}dA,\ K_{\alpha\beta^y}=\int_A N_\alpha N_{\beta,y}dA,\ K_{\alpha\beta\gamma^x}=\int_A N_\alpha N_\beta N_{\gamma,x}dA$$

$$K_{\alpha\beta\gamma^y}=\int_A N_\alpha N_\beta N_{\gamma,y}dA,\ K_{\alpha\beta}=\int_A N_\alpha N_\beta dA,\ S_{\alpha\beta^{xx}}=\int_A N_{\alpha,x}N_{\beta,x}dA$$

$$S_{\alpha\beta^{xy}}=\int_A N_{\alpha,y}N_{\beta,y}dA,\ M_{\alpha\mu^x}=\int_A H_\alpha H_{\mu,x}dA,\ M_{\alpha\mu^y}=\int_A H_\alpha H_{\mu,y}dA$$

$$Q_{\alpha^u}=\int_{S_0}N_\alpha S_x dS_0,\ Q_{\alpha^v}=\int_{S_0}N_\alpha S_y dS_0,\ Q_{\alpha^\theta}=\int_{S_w}N_\alpha q_w dS_w$$

$$K_\alpha=\int_A N_\alpha dA.$$

These element matrices are evaluated in closed-form ready for numerical simulation. Details of the derivation for these element matrices are omitted herein for brevity. The derived finite element equations, Eqs. (9)-(12), are nonlinear and are solved by applying the Newton-Raphson iteration technique by first writing the unbalanced values from the set of the finite element Eqs. (9)-(12) as,

$$F_{\alpha^p}=K_{\alpha\beta^x}U_\beta+K_{\alpha\beta^y}V_\beta$$

$$F_{\alpha^u}=K_{\alpha\beta\gamma^x}U_\beta U_\gamma+K_{\alpha\beta\gamma^y}V_\gamma U_\gamma+M_{\alpha\mu^x}P_\mu+(S_{\alpha\beta^{xx}}+S_{\alpha\beta^{yy}})U_\beta-\left(\frac{Ra_E}{Pr}sin\Phi\right)K_{\alpha\beta}\theta_\beta-Q_{\alpha^u}$$

$$F_{\alpha^v} = K_{\alpha\beta\gamma^x} U_\beta V_\gamma + K_{\alpha\beta\gamma^y} V_\gamma V_\gamma + M_{\alpha\mu^y} P_\mu + (S_{\alpha\beta^{xx}} + S_{\alpha\beta^{yy}}) V_\beta - \left(\frac{Ra_E}{Pr} cos\Phi\right) K_{\alpha\beta}\theta_\beta - Q_{\alpha^v}$$

$$F_{\alpha^\theta} = K_{\alpha\beta\gamma^x} U_\beta \theta_\gamma + K_{\alpha\beta\gamma^y} V_\beta \theta_\gamma + \frac{1}{Pr}(S_{\alpha\beta^{xx}} + S_{\alpha\beta^{yy}})\theta_\beta - \left(\frac{Ra_I}{Ra_E Pr}\right) K_\alpha - Q_{\alpha^\theta}$$

GRID SENSITIVITY TEST

The numerical procedure used to solve the governing equations for the present work is the finite element based adapting meshing technique. The application of this technique is well documented in[31]. It provides the smooth solutions at the interior domain including the corner regions. A nine nodded triangular elements are used in this paper. Solutions were assumed to converge when the following convergence criteria was satisfied for every dependent variables at every point in the solution domain

$$\left|\frac{\psi_{new} - \psi_{old}}{\psi_{old}}\right| \le 10^{-6}$$

where ψ represents a dependent variable *U*, *V*, *P*, and *θ*.

In order to obtain grid independent solution, a grid refinement study is performed for $Ra_E = 10^3$, $Ra_I = 10^5$, and $\Phi = 0°$. Figure 2 shows the convergence of the average Nusselt number, *Nu*, at the heated surface with grid refinement. It is observed that grid independence is achieved with 6392 elements where there is insignificant change in *Nu*.

CODE VALIDATION

In order to validate the numerical code, the results are compared with those reported by Shim and Hyun[20] and Oztop and Bilgen[19]. It is seen from Table 1 that average Nusselt numbers are in good agreement. The streamlines and isotherms of the present investigation for $Ra_E = 10^5$ and $Ra_I = 10^7$ as shown in Fig. 3 are analogous to those obtained by Shim and Hyun[20]. This accuracy provides credence to the present computation.

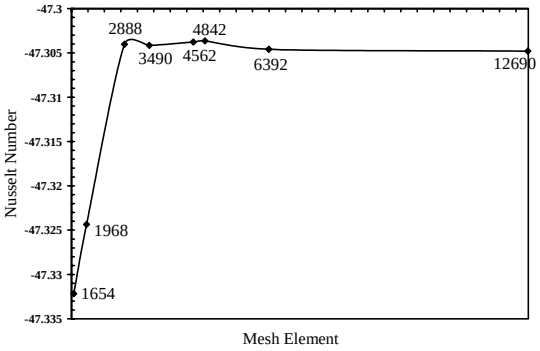

Figure 2: Convergence of *Nu* with Grid Refinement for $Ra_E = 10^3$, $Ra_I = 10^5$ & $\Phi = 0°$.

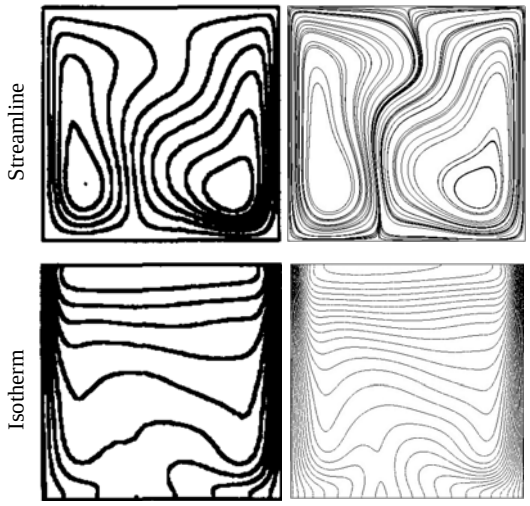

Fig. 3: Comparison of flow and thermal fields

Table 1: Comparison of average Nusselt number with Shim and Hyun[20] and Oztop and Bilgen[19].

Nu				
Ra_I	Ra_E	Shim and Hyun[20]	Oztop and Bilgen[19]	Present
10^6	10^5	– 0.01	+ 0.1	– 0.1
10^7	10^5	– 66.0	– 59.0	– 43.02

RESULTS AND DISCUSSION

In this investigation, streamlines and isotherms inside the inclined square enclosure and the average Nusselt number distribution at the heated surface have been examined and discussed for the external Rayleigh number, Ra_E, varied from 10^3 to 10^6, and the internal Rayleigh number, Ra_I, varied from 10^5 to 10^8. The working fluid is chosen as air with Prandtl number, $Pr = 0.71$. The inclination angle is ranging from 0° to 30°.

Thermo-fluid characteristics

The evolution of flow, when the effect of internal heat generation is dominated for different inclination angles and $Ra_E = 10^3$ is depicted in Fig. 4. When there is no tilting effect of the enclosure, the flow and thermal fields experience the strong influence of internal heat generation for $Ra_I = 10^5$ and $Ra_E = 10^3$. Pre-existing external heating is fully overwhelmed by the relative effect of internal heat generation. The whole cavity is occupied by two recirculating cells; i.e. both counter-clockwise and clockwise cells near the hot and cold side walls due to the negative and positive buoyancy effect respectively. The sinking motion near the cold wall is intensified compared to that near the hot wall due to the differential buoyancy effect. With an increase in Ra_I, the circulations are turned into irregular shape due to vigorous sinking motion causing from the higher interior temperatures. Thereby heat transfer rate is enhanced. At $\Phi = 30^o$, lower value of Ra_I

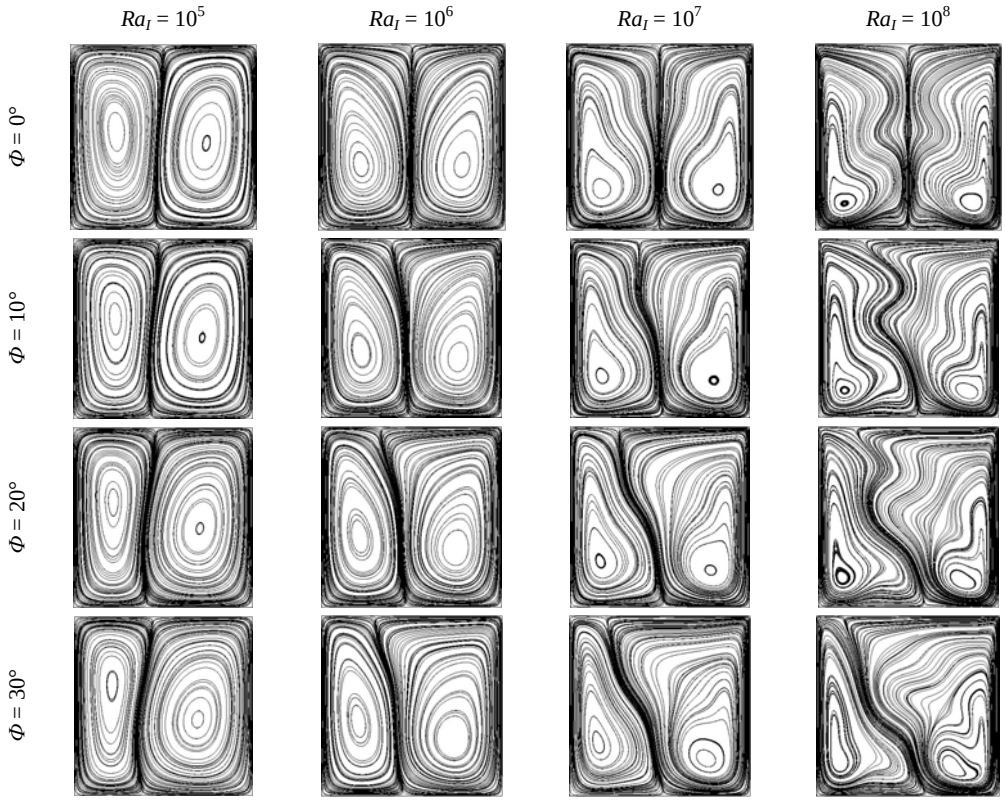

Fig. 4: Variation of streamlines for external Rayleigh number, $Ra_E = 10^3$.

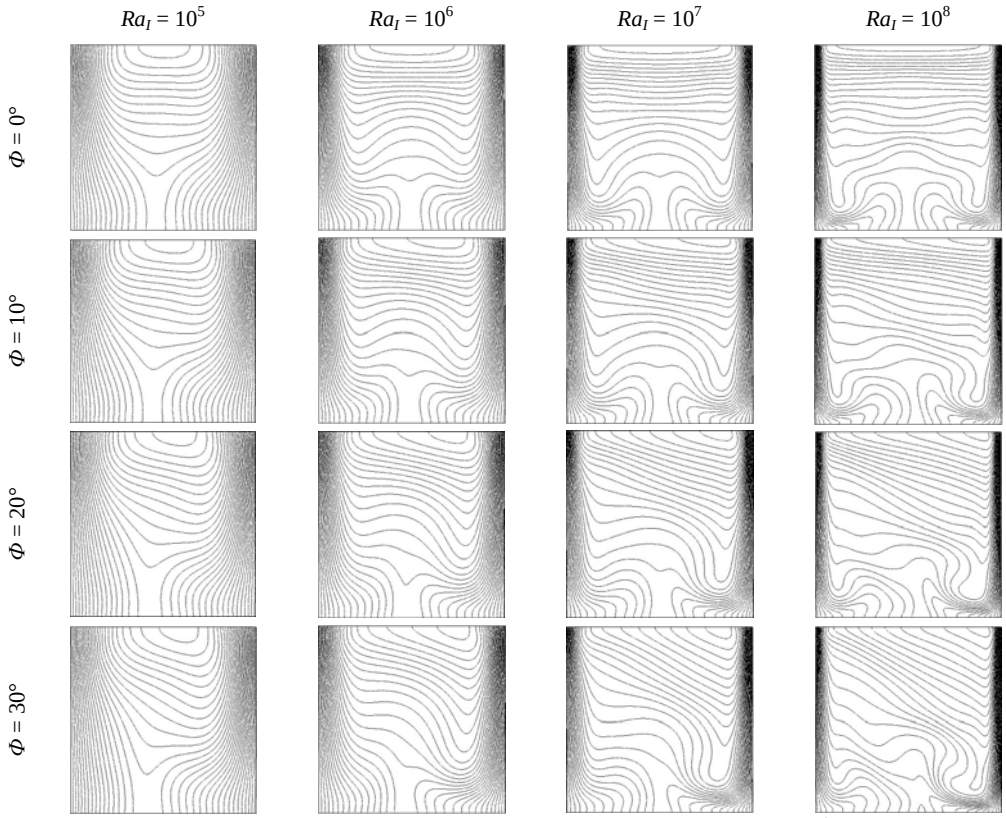

Fig. 5: Variation of isotherms for external Rayleigh number, $Ra_E = 10^3$.

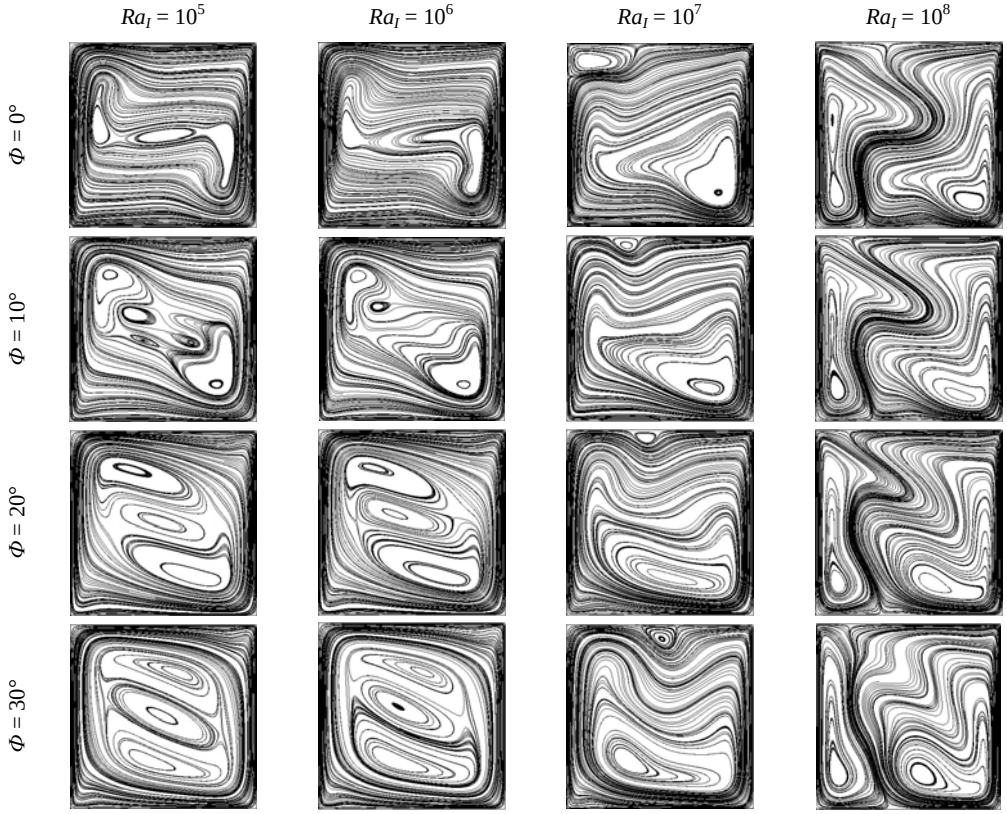

Fig. 6: Variation of streamlines for external Rayleigh number, $Ra_E = 10^6$.

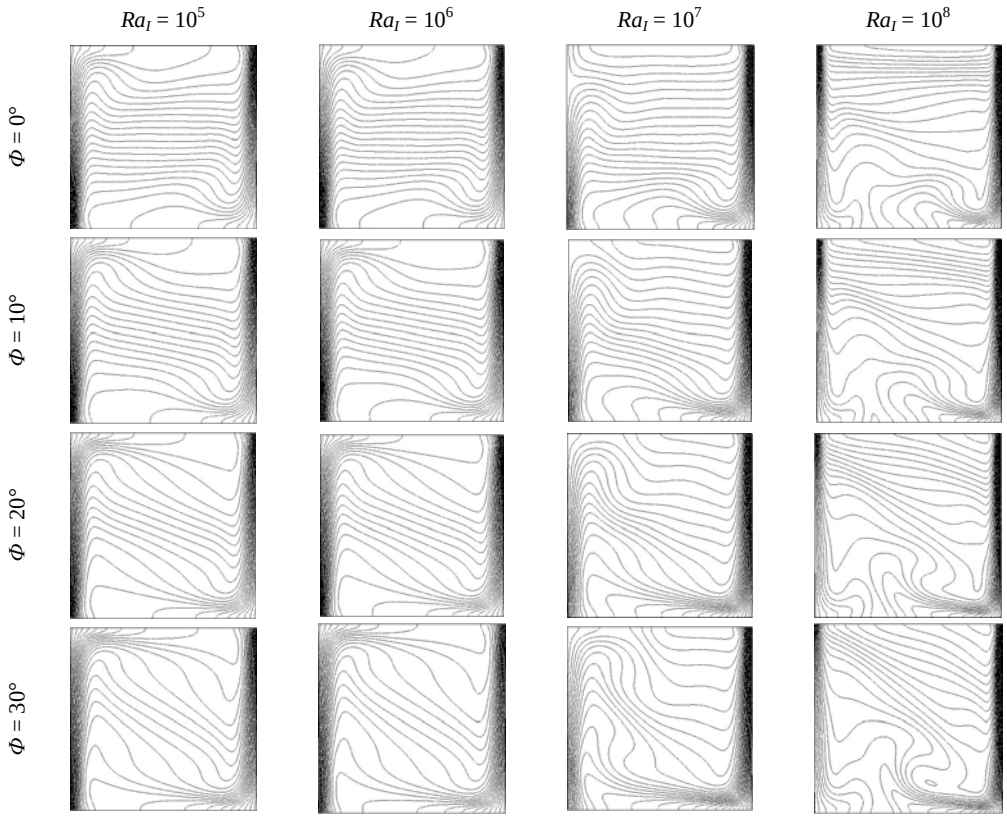

Fig. 7: Variation of isotherms for external Rayleigh number, $Ra_E = 10^6$.

(but sufficiently strong for generating the internal heat generation effect), the flow pattern has different nature with fluid moving upwards in the interior of the enclosure and moving down both the hot and cold walls. It is remarkable that the sinking flow along the hot wall is sturdy whereas it is weaker along the cold wall. This is because the x-component of buoyancy effect due to external heating opposes the flow due to internal heating moving down the hot surface and aids the flow due to internal heating moving down the cold surface. As the inclination angle increases, the effect of x-component of buoyancy becomes profound. For this reason, the downward flow over the cold surface increases in size and becomes faster while the sinking flow near the hot wall is reduced in size and becomes slower.

The upshot of the internal heat generation and the inclination angle of the cavity on the thermo-fluid scenario for $Ra_E = 10^3$ are depicted in Fig. 5. The isotherms represent that the thermal boundary layers near the hot and cold walls increases and is concentrated as the effect of the internal heat generation increases. In the presence of relatively low value of Ra_I at $\Phi = 0^o$, isotherms are almost linear at the upper part of the cavity, indicating diffusion dominated heat transfer but at lower part of the interior of cavity convection is liable for the heat transport phenomenon. At higher value of Ra_I, isotherms tend to be horizontally uniform and vertically linear at the upper portion of the enclosure. However, in the bottom part of the cavity interior, in line with the emergence of two circulating cells of comparable magnitude, the isotherms are divided into two groups. The total thermal energy in the cavity is on increase. It should be marked that the boundary layer behavior at the hot and cold walls decreases as the inclination angle is increased. With the increment of the tilting angle, the isotherms near the bottom part of the cold wall spread and rigorous plume formation is found at higher value of Ra_I.

Considerations are given to the cases when the effects of external heating and internal heat generation are comparable. Figure 6 is illustrative of the sequences of flow and thermal fields for such cases. Performing order of magnitude analysis on $Ra_I = 10^5$ and $Ra_E = 10^6$, implies that the relative impact of internal heat generation is minor. The flow is attributed by the presence of a single clockwise circulation cell, which occupies much of the cavity and a secondary and a tertiary vortices are formed inside the cavity. Increased impact of the internal heat generation provides an aiding (or opposing) buoyancy effect to the fluid in the vicinity of the cold (or hot) wall. The sinking (or rising) motion in the boundary layer on the cold (or hot) side wall is enhanced (or hindered). At higher value of Ra_I, the hindrance of the flow is so strong that a sinking motion is established near the hot wall. Thus two irregular circulating cells of differential strength and opposite directions of motion are introduced. The irregularity of the circulating cells is appeared due to the chaotic flow, which in turns marks the better convective thermal performance. The convective heat transfer is dictated by the inclination angle. Increasing the inclination angle gives a complex discernible flow field scenario until the Ra_I is equal to Ra_E. At small value of Φ, five vortices of very minute in size and strength are visible at the interior of the cavity, but the primary circulation of clockwise direction of motion through the hot wall to the cold wall is still domineer. As Ra_I increases, those small vortices are merged to the primary vortex of relatively higher intensity of circulation than that at low Ra_I. For higher value of Ra_I ($Ra_I = 10^8$), two irregular circulations are observed. The circulation cell near the vicinity of the cold wall is intensified at the bottom part of the cavity. Thereby heat is solely transferred by buoyancy-driven-convection mechanism. Further increase in Φ reveals that the convective currents are overwhelmed by the diffusive currents at low Ra_I.

The influence of the internal heat generation and the inclination angle on the fluid and thermal fields inside a square cavity is presented in Fig. 7, while the higher external heating is imposed. At $\Phi = 0^o$, the isotherms represent that the diffusion is the principal mode of heat transfer when relative impact of Ra_I is small. At higher Ra_I, the isotherms remain unaltered at the upper part but vigorous plume formation appears at the lower part of the cavity being a sign of the better convection heat transfer. At $\Phi = 30^o$, the isotherms are diagonally linear even at low Ra_I which means that the buoyancy effect is suppressed by the diffusion effect. Prolonged clusters of isotherms near the bottom wall suppress the plume formation at higher value of Ra_I resulting relatively low thermal performance compared to that of the zero inclination angles.

Heat Transfer Characteristics

Figure 8 illustrates the variation of average Nusselt number for different values of internal heat generation and the inclination angles at different values of external heating. In the presence of internal heat sources, the value of *Nu* along the hot side wall is governed by the direction and strength of the flow adjacent to the hot wall. At each Ra_I depending on Ra_E, part of the interior hot fluid flows downward along the hot surface forming a counter-direction circulation near the hot wall. Thereby the average Nusselt number along hot wall becomes negative which means that the hot wall absorbs the heat from the interior higher temperature fluid. In general, average Nusselt number remains invariant to the Ra_I ranging from 10^5 to 10^6. Increasing the impact of internal heat generation causes the rapid rise in average Nusselt number. Maximum thermal performance is obtained for the lower value of external heating. Moreover a discernible thermal behavior is observed in Fig. 8(d). Since the order of magnitude of external heating is comparable to internal heat generation, the positive value of average Nusselt number marks that there is rising motion near the hot wall though the circulation feels retardation due to the buoyancy effect generated by internal heat generation. Therefore, as Ra_I increases in magnitude, the average Nusselt number decreases up to certain value of Ra_I ($Ra_I \sim 3\times10^7$). After that it increases in negative direction indicating the sinking motion near the hot side wall.

CONCLUSION

Natural convection in a tilted square enclosure subjected to the differential heating boundary conditions and containing internal energy sources has been investigated using finite element discretizition scheme. Results indicate that in the presence of relatively weak external heating mode, the diffusion heat transfer is prominent for the lower value of internal heat generation whereas the convection outweighs the diffusion for the higher value of internal energy. It is noticed that the convective currents always prevail at the bottom part of the cavity whatever its magnitude is. When the higher differential temperature is imposed at the side walls of the cavity, the relative value of external energy is amplified

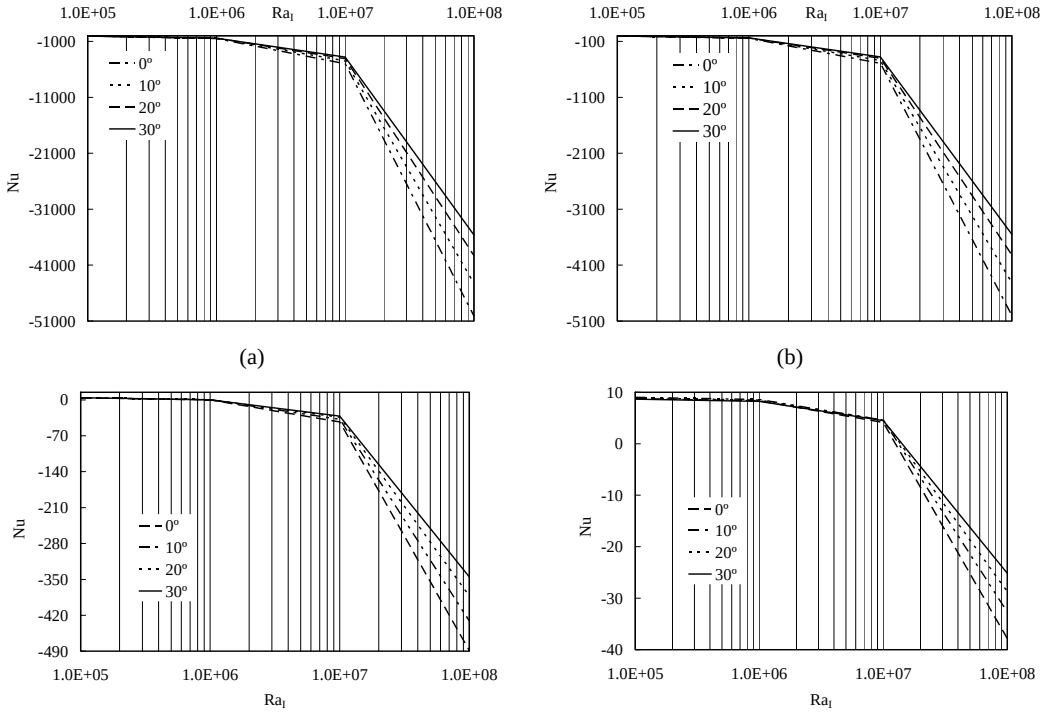

Fig. 8: Variation of the average Nusselt number along with Ra_I for (a) $Ra_E = 10^3$, (b) $Ra_E = 10^4$, (c) $Ra_E = 10^5$ and (d) $Ra_E = 10^6$

which in turn accelerates the convective currents even at the lower value of internal heat generation. Average Nusselt number is decreased with an increment of the tilted angle. In general, optimum heat transfer performance is obtained at zero inclination angle. The synopsis is that relatively weak external heating mode yields the better thermal performance for all values of internal energy generated within the fluid.

REFERENCES

1. Ostrach, S., 1972, "Natural Convection in Enclosures," In Advances in Heat Transfer, (eds. J. P. Hartnett and T F. Irvine), Vol. 8, pp. 161–227.

2. Catton, I., 1978, "Natural Convection in Enclosures," Proc. 6th Int. Heat Transfer Conf., Vol. 2, pp. 13–31.

3. Kulack, F. A., Catton, I., Chen, C. F., and Edwards, D. K., 1982, "Fluid Layers," Proc. of a Workshop on Natural Convection, (eds. Yang, K. T. and Lioyd, J. R.) July 18–21, Breckenridge, Colorado.

4. Baker, L., Faw, R. E., and Kulaeki, F. A., 1976, "Post Accident Heat Removal - Part 1: Heat Transfer within an Internally Heated, Non-boiling Liquid Layer," Nucl. Sci. Eng., Vol. 61, pp. 222–230.

5. Cheung, F. B., 1978, "Correlation Equation for Turbulent Thermal Convection in a Horizontal Layer Heated Internally and From Below," J. Heat Transfer, Vol. 100, pp. 416–422.

6. Kikuehi, Y., Kawasaki, T., and Shiyoma, T., 1982, "Thermal Convection in a Horizontal Fluid Layer Heated Internally and From Below," Int. J. Heat Mass Transfer, Vol. 25, pp. 363–370.

7. Boon-Long, P., Lester, T. W., and Faw, R. E., 1979, "Convective Heat Transfer in an Internally Heated Horizontal Fluid Layer with Unequal Boundary Temperatures," Int. J. Heat Mass Transfer, Vol. 22, pp. 437–445.

8. Suo-Anttila, A. J., and Catton, I., 1975, "The Effect of a Stabilizing Temperature Gradient on Heat Transfer from a Molten Fuel Layer with Volumetric Heating," J. Heat Transfer, Vol. 97, pp. 544–548.

9. Suo-Anttila, A. J., and Catton, I., 1976, "An Experimental Study of a Horizontal Layer of Fluid with Volumetric Heating and Unequal Surface Temperatures," 16th National Heat Transfer Conference, St. Louis, Paper No. AICHE–5.

10. Steinberner, U., Reinke, H. H., 1978, "Turbulent Buoyancy Convection Heat Transfer with Internal Heat Source," *Proc., 6th International Heat Transfer Conference*, Toronto, Canada, August 7–11, Hemisphere Publishing Corp., Washington, DC, NC-21, Vol. 2, pp. 305–311.

11. Kulacki, F. A., and Goldstein, R. J., 1972, "Thermal Convection in a Horizontal Fluid Layer with Uniform Volumetric Energy Sources," J. Fluid Mech., Vol. 55, pp. 271–287.

12. Lee, J. H., and Goldstein, R. J., 1988, "An Experimental Study on Natural Convection Heat Transfer in an Inclined Square Enclosure Containing Internal Energy Sources," ASME J. Heat Transfer, Vol. 110, pp. 345–349.

13. Acharya, S., Goldstein, R. J., 1985, "Natural Convection in an Externally Heated Vertical or Inclined Square Box Containing Internal Energy Sources," ASME J. Heat Transfer Vol. 107, pp. 855–866.

14. Emara, A. A., Kulacki, F. A., 1980, "A Numerical Investigation of Thermal Convection in a Heat-generating Fluid Layer," ASME J. Heat Transfer, Vol. 102, pp. 531–537.

15. Rahman, M., and Sharif, M. A. R., 2003, "Numerical Study of Laminar Natural Convection in Inclined Rectangular Enclosures of Various Aspect Ratios," Numer. Heat Transfer A, Vol. 44, pp. 355–373.

16. Kawara, Z., Kishiguchi, I., Aoki, N., and Michiyoshi, I., 1990, "Natural Convection in a Vertical Fluid Layer with Internal Heating," *Proc., 27th National Heat Transfer Symposium*, Japan, vol. II, pp. 115–117.

17. Fusegi, T., Hyun, J. M., and Kuwahara, K., 1992, "Natural Convection in a Differentially Heated Square Cavity with Internal Heat Generation," Numer. Heat Transfer A, Vol. 21, pp. 215–229.

18. Fusegi, T., Hyun, J. M., and Kuwahara, K., 1992, "Numerical Study of Natural Convection in a Differentially Heated Cavity with Internal Heat Generation: Effects of the Aspect Ratio," J. Heat Transfer, Vol. 114, pp. 773–777.

19. Oztop, H., and Bilgen, E., 2006, "Natural Convection in Differentially Heated and Partially Divided Square Cavities with Internal Heat Generation," Int. J. Heat Fluid Flow.

20. Shim, Y. M., and Hyun, J. M., 1997, "Transient Confined Natural Convection with Internal Heat Generation," Int. J. Heat Fluid Flow, Vol. 18, pp. 328–333.

21. Baytas, A. C., 1996, "Buoyancy-driven Flow in an Enclosure Containing Time Periodic Internal Sources," Heat Mass Transfer, Vol. 31, pp. 113–119.

22. Liaqat, A., and Baytas, A. C., 2001, "Conjugate Natural Convection in a Square Enclosure Containing Volumetric Sources," Int. J. Heat Mass Transfer, Vol. 44, pp. 3273–3280.

23. Kulacki, F. A., and Goldstein, R. J., 1975, "Hydrodynamic Instability in Fluid Layers With Uniform Volumetric Energy Sources," Appl. Sci. Res., Vol. 31, pp. 81–109.

24. Drazin, P. G., and Reid, W. H., 1981, "Hydrodynamic Stability," Cambridge University Press, London.

25. May, H. O., 1991, "A Numerical Study on Natural Convection in an Inclined Square Enclosure Containing Internal Heat Resources," Int. J. Heat Mass Transfer, Vol. 34, pp. 919–928.

26. Di Piazza, I., and Ciofalo, M., 2000, "Low-Prandtl Number Natural Convection in Volumetrically Heated Rectangular Enclosures I, AR = 4," Int. J. Heat Mass Transfer, Vol. 43, pp. 3027–3051.

27. Arcidiacono, S., Di Piazza, I., and Ciofalo, M., 2001, "Low-Prandtl Number Natural Convection in Volumetrically Heated Rectangular Enclosures II Square Cavity, AR = 1," Int. J. Heat Mass Transfer, Vol. 44, pp. 537–550.

28. Arcidiacono, S., and Ciofalo, M., 2001, "Low-Prandtl Number Natural Convection in Volumetricaly Heated Rectangular Enclosures III Shallow Cavity, AR = 0.25," Int. J. Heat Mass Transfer, Vol. 44, pp. 3053–3065.

29. Daniels, P. G., and Jones, O. K., 1998, "Convection in a Shallow Rectangular Cavity Due to Internal Heat Generation," Int. J. Heat Mass Transfer, Vol. 41, pp. 3979–3987.

30. Joshi, M. V., Gaitonde, U. N., and Mitra, S. K., 2004, "Analytical Study of Natural Convection in a Cavity With Volumetric Heat Generation," *Proc. ASME Heat Transfer/Fluids Engineering Summer Conference*, HTFED 2004–56302.

31. Dechaumphai, P., and Kanjanakijkasem, W., 1999, "A Finite Element Method for Viscous Incompressible Thermal Flows," Science Asia, Vol. 25, pp. 165-172.